Rapid Communications

Unraveling the non-Hermitian skin effect in dissipative systems

Stefano Longhi *

Dipartimento di Fisica, Politecnico di Milano, Piazza L. da Vinci 32, I-20133 Milano, Italy
and IFISC (UIB-CSIC), Instituto de Fisica Interdisciplinar y Sistemas Complejos, E-07122 Palma, Spain

(Received 28 August 2020; revised 22 October 2020; accepted 23 October 2020; published 5 November 2020)

The non-Hermitian skin effect, i.e., eigenstate condensation at the edges in lattices with open boundaries, is an exotic manifestation of non-Hermitian systems. In Bloch theory, an effective non-Hermitian Hamiltonian is generally used to describe dissipation, which, however, is not norm preserving and neglects quantum jumps. Here it is shown that in a self-consistent description of the dissipative dynamics in a one-band lattice, based on the stochastic Schrödinger equation or Lindblad master equation with a collective jump operator, the skin effect and its dynamical features are washed out. Nevertheless, both short- and long-time relaxation dynamics provide a hidden signature of the skin effect found in the semiclassical limit. In particular, relaxation toward a maximally mixed state with the largest von Neumann entropy in a lattice with open boundaries is a manifestation of the semiclassical skin effect.

DOI: 10.1103/PhysRevB.102.201103

Introduction. Dissipative lattices, where energy or particle number are not conserved, show intriguing topological properties and phase transitions that are attracting a great interest in different areas of physics [1–65]. Band theory describes open systems by non-Hermitian Hamiltonians [14,17,25,26,42,46] and predicts a wealth of exotic features such as a strong sensitivity of the energy spectrum on boundary conditions [11,12,15,17], the non-Hermitian skin effect (NHSE), i.e., the condensation of bulk modes at the edges [13–18,46,54], and breakdown of bulk-boundary correspondence based on Bloch topological invariants [6,12–15,30–36,47–50,52]. However, on a fundamental level the non-Hermitian description generates a nonunitary dynamics and ignores quantum jumps. The natural description of quantum dynamics in open systems is provided by master equations in Lindblad form or stochastic Schrödinger equations, where stochastic terms ensure unitary time evolution. This has motivated the search for a topological classification of dissipative systems and for exotic phenomena such as the skin effect beyond non-Hermitian band theory [24,56,61,62]. Recently, topological classifications of dissipative systems based on the complex spectrum of the Lindbladian superoperator or on quantum jump dynamics [56,61] have been suggested, and the prediction of important phenomena, such as the boundary-dependent damping dynamics and the Liouvillian skin effect [24,62], have been disclosed. An open question is whether signatures of the NHSE in non-Bloch band theory persist when considering stochastic terms or quantum jumps, i.e., beyond a mean-field theory.

In this Rapid Communication it is shown that the NHSE of non-Hermitian band theory and its dynamical signatures are washed out in a minimal model of stochastic dynamics which restores a unitary time evolution. Nevertheless, both short- and long-time relaxation dynamics provide hidden signatures of the NHSE. In particular, in the one-band limit the relaxation toward a maximally mixed state with the largest von Neumann entropy under open boundaries is the manifestation of the semiclassical NHSE.

Dissipative dynamics and skin effect. In the framework of single-particle Bloch theory, a one-band dissipative lattice made of N sites under either periodic (PBC) or open (OBC) boundary conditions is described in Wannier basis $|n\rangle$ by an effective $N \times N$ non-Hermitian matrix Hamiltonian $\hat{H}_{eff}$, which can be written as the sum of Hermitian $\hat{H}$ and anti-Hermitian $i\hat{A} = -(i/2)\hat{P}^2$ parts, i.e.,

$$\hat{H}_{eff} = \hat{H} - (i/2)\hat{P}^2 \tag{1}$$

with $\hat{H}^\dagger = \hat{H}$ and $\hat{P}^\dagger = \hat{P}$ for a purely dissipative lattice. Under PBC, in momentum space the Hamiltonian is diagonal and takes the form

$$H_{eff}(k) = H(k) - (i/2)P^2(k), \tag{2}$$

where k is the Bloch wave number and $P(k)$ can be taken as a non-negative function. Here we assume that the Hermitian dynamics, described by $\hat{H}$, shows time-reversal symmetry so that $H(-k) = H(k)$ in momentum space and $\hat{H}^T = \hat{H}$ in physical space. For any Hermitian Hamiltonian, the bulk energy spectrum in the thermodynamic limit $N \to \infty$ becomes independent of boundary conditions, and the energy spectra may differ just for the appearance of isolated energies corresponding to edge states under OBC. However, for a generic non-Hermitian Hamiltonian the bulk eigenenergies under PBC and OCB rather generally differ considerably in the thermodynamic limit owing to the NHSE [13–18]. In particular, the energy spectrum of $\hat{H}_{eff}$ is different for PBC and OBC whenever $P(-k) \neq P(k)$, i.e., the NHSE does not arise provided that the system possesses the additional symmetry $\hat{P}^T = \hat{P}$. In fact, for $P(-k) \neq P(k)$ the PBC energy

* stefano.longhi@polimi.it

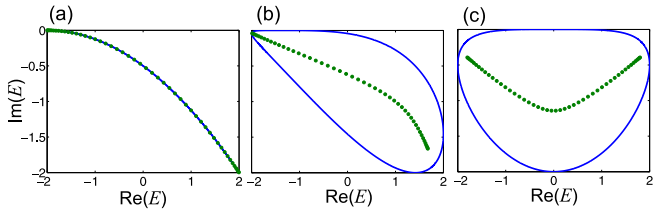

FIG. 1. Energy spectrum in complex plane of the non-Hermitian lattice, defined by Eqs. (1) and (3), for $J = R = 1$, $T = 0$ and for a few increasing values of the phase φ: (a) $\varphi = 0$, (b) $\varphi = \pi/4$, and (c) $\varphi = \pi/2$. Solid curves refer to PBC, while circles refer to OBC in a lattice comprising $N = 50$ sites. The NHSE appears in (b) and (c), where PBC and OBC energy spectra are distinct.

spectrum describes a closed loop in the complex energy plane with a finite number of self-intersections [66], while under OBC the energy spectrum must collapse to one (or a set of) closed curves in the interior of the closed loop [17,29,63]. As an example, PBC and OBC bulk energy spectra for the dissipative lattice with

$$H(k) = 2J\cos k + 2T\cos(2k), \quad P(k) = R[1+\cos(k+\varphi)] \tag{3}$$

are depicted in Fig. 1. Note that a nonvanishing phase $\varphi \neq 0$, breaking the symmetry $P(-k) = P(k)$, results in the NHSE. The description of dissipation based on the use of $\hat{H}_{eff}$ in the Schrödinger equation suffers from the fact that the state vector $|\psi(t)\rangle$ undergoes a nonunitary evolution and neglects quantum jumps. As such a description can be regarded as a semiclassical limit of the Markovian dynamics of the open quantum system and can naturally appear in postselection of quantum trajectories [67,68], increasing attention is currently devoted to unveiling NHSE beyond the semiclassical limit [24,56,61,62]. A unitary dynamics is restored by considering a *stochastic* Schrödinger equation, where stochastic terms are added to the deterministic evolution of $|\psi(t)\rangle$ so as to preserve the norm [69]. This description is equivalent to the use of a master equation in Lindblad form [69]. As the choice of the stochastic terms (i.e., jump operators) is not unique [69,70] and a detailed microscopic knowledge of the system-bath coupling would be required, here we focus our attention on a model that exploits a single nonlocal jump operator [67], corresponding to the stochastic Schrödinger equation (in the Itô interpretation [69,71])

$$id|\psi(t)\rangle = \hat{H}_{eff}|\psi(t)\rangle dt + \xi(t)\hat{P}|\psi(t)\rangle dt, \tag{4}$$

where $\xi(t)$ is a zero-mean delta-correlated white noise, i.e., $\overline{\xi(t)} = 0$ and $\overline{\xi(t)\xi(t')} = \delta(t-t')$. Note that the mean value $\overline{|\psi(t)\rangle}$, averaged over all realizations of noise, evolves as $\overline{|\psi(t)\rangle} = \exp(-it\hat{H}_{eff})\overline{|\psi(0)\rangle}$, corresponding to the mean-field (or semiclassical) dynamics with effective non-Hermitian Hamiltonian $\hat{H}_{eff}$. The associated Lindblad master equation for the density operator $\hat{\rho} = \overline{|\psi(t)\rangle\langle\psi(t)|}$ involves a single jump operator $\hat{P} = \hat{P}^\dagger$ and reads [69,70]

$$\frac{d\hat{\rho}}{dt} = -i[\hat{H},\hat{\rho}] - \frac{1}{2}\left(\hat{P}^2\hat{\rho} + \hat{\rho}\hat{P}^2 - 2\hat{P}\hat{\rho}\hat{P}\right) \equiv \mathcal{L}\hat{\rho}, \tag{5}$$

where $\mathcal{L}$ is the Liouvillian superoperator. We stress that this model with a collective jump operator may not be sufficient to fully capture the underlying dissipative process; however, it has been suggested as a minimal description (involving a single jump operator) of the open system dynamics beyond the semiclassical limit [67]. Also, the stochastic or master equation approach can describe system dynamics under classical noise [69,72,73], where the model of Eq. (4) can be realized.

Relaxation dynamics. The spectrum and corresponding N^2 eigenmodes of the Liouvillian superoperator $\mathcal{L}$ are rather generally different for lattices with PBC and OBC, so that relaxation and decoherence dynamics are boundary dependent [24]. In particular, the exponential localization of the eigenmodes of $\mathcal{L}$ at the edges results in so-called Liouvillian skin effect [62], which is responsible for slowing down of relaxation processes without gap closing. Here we consider a different scenario, where the semiclassical NHSE is washed out by the stochastic dynamics and $\mathcal{L}$ does not show skin modes. The main result of this work is that the semiclassical NHSE can be nevertheless unraveled by looking at the relaxation dynamics both at short and long time scales. Let us first consider the *short-time* (bulk) relaxation dynamics, where initial excitation is spatially confined far from the boundaries and edge effects are negligible. In this case Eq. (4) can be solved in momentum space, where all operators are diagonal. After expanding the state vector in Bloch basis as $|\psi(t)\rangle = \int_{-\pi}^{\pi} dk\, \Psi(k,t)|k\rangle$, where k is the Bloch wave number and $|k\rangle \equiv (1/\sqrt{2\pi})\sum_n \exp(ikn)|n\rangle$ the Bloch basis, one obtains

$$\Psi(k,t) = \Psi(k,0)\exp[-iH(k)t - iP(k)W(t)], \tag{6}$$

where $W(t)$ is a Wiener process with $\overline{W(t)} = 0$ and $\overline{W^2(t)} = t$. The corresponding evolution of the density operator in Bloch basis, $\rho_{k,k'}(t) = \langle k|\rho|k'\rangle$, reads

$$\rho_{k,k'}(t) = \overline{\Psi(k,t)\Psi^*(k',t)} = \rho_{k,k'}(0)\exp[iG(k,k')t], \tag{7}$$

where we have set $G(k,k') = H(k') - H(k) + (i/2)[P(k') - P(k)]^2$. The signature of the semiclassical NHSE in the short time scale is clearly observed looking at the relaxation dynamics of density matrix elements $\rho_{n,m}(t) = \langle n|\hat{\rho}|m\rangle$ in Wannier basis. In particular, assuming an initial pure state with excitation at site $n = 0$, i.e., $\rho_{n,m}(0) = \delta_{n,0}\delta_{m,0}$, one has (see [70] for details)

$$\rho_{n,m}(t) = \frac{1}{4\pi^2}\iint dk\, dk' \exp[ikn - ik'm + iG(k,k')t]. \tag{8}$$

For $P(-k) = P(k)$, i.e., when $\hat{H}_{eff}$ does not show the NHSE, the relaxation process is highly symmetric around $n = m = 0$, namely, $\rho_{-n,m} = \rho_{n,-m} = \rho_{-n,-m} = \rho_{n,m}$ owing to the even symmetry of the spectral term $G(k,k')$ under momentum inversion. This means that coherence is created and maintained during the relaxation process. On the other hand, for $P(-k) \neq P(k)$, i.e., when $\hat{H}_{eff}$ shows the NHSE, using a multivariate saddle-point method [74] it can be shown [70] that the slowest decaying terms are those along the main diagonal $n = m$, i.e., "populations," while terms along the antidiagonal $n = -m$, i.e., "coherences," decay faster. Such a distinct behavior in relaxation dynamics is illustrated in Fig. 2 for the model defined by Eq. (3). Note that the ballistic spreading of populations, i.e., of $\rho_{n,n}(t)$, is symmetric at around $n = 0$, while in the semiclassical limit one would

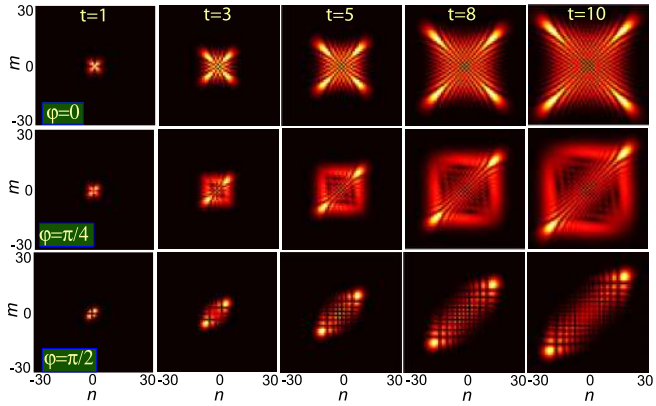

FIG. 2. Bulk (short-time) relaxation dynamics in the dissipative lattice defined by Eq. (3) for three values of the phase φ (0, $\pi/4$, and $\pi/2$). The panels show snapshots of the density matrix $|\rho_{n,m}(t)|$ in Wannier basis at successive times on a pseudocolor map. The initial state is the pure state $\rho(0) = |0\rangle\langle 0|$, corresponding to a particle localized at site $n = 0$. Lattice parameters are $J = R = 1$ and $T = 0$.

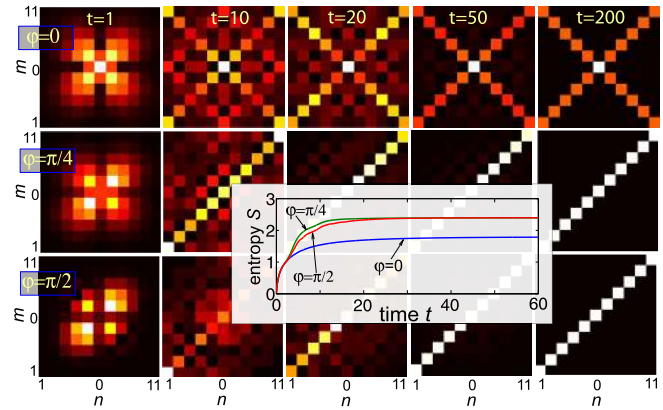

FIG. 3. Same as Fig. 2, but in a lattice comprising $N = 11$ sites with open boundaries. Initial state is $\hat{\rho}(0) = |6\rangle\langle 6|$. Inset: evolution of the von Neumann entropy S for the three phases $\varphi = 0$, $\pi/4$, and $\pi/2$. The long-time asymptotic state is a maximally mixed state, corresponding to the largest value of entropy $S = \ln N$, except for $\varphi = 0$.

expect a *unidirectional* flow when $\hat{H}_{eff}$ shows the NHSE [29], as illustrated in Supplemental Material Fig. S.1 of [70]. This means that quantum jumps fully change the spreading features of excitation along the lattice as compared to the mean-field model. Yet, the signature of the semiclassical NHSE is visible looking at the coherences, which decay faster leading to a characteristic *elongated* spreading pattern when the systems show the NHSE in the semiclassical limit.

The other hidden signature of the semiclassical NHSE is found looking at the long-time relaxation dynamics, where edge effects cannot be neglected. In this case the relaxation process is established by the nondecaying eigenvectors of the Liouvillian superoperator. Interestingly, more than one stationary state can exist under certain symmetries of $\mathcal{L}$ [75–77], which in our model depend on the symmetries of $\hat{H}$ and $\hat{P}$. The N^2 eigenvalues λ_l of $\mathcal{L}$ always appear in complex conjugate pairs and satisfy the condition $\mathrm{Re}(\lambda_l) \leqslant 0$. If $\mathcal{L}$ shows a single nondecaying eigenvector $\hat{\rho}^{(s)}$ with zero eigenvalue, the system relaxes toward the stationary state $\hat{\rho}^{(s)}$. For the master equation (5) it can be readily shown that the state $\rho^{(s)}_{n,m} = (1/N)\delta_{n,m}$ is an eigenvector of $\mathcal{L}$ with zero eigenvalue. Such a stationary state corresponds to a maximally mixed state, with von Neumann entropy $S(\hat{\rho}) = -\mathrm{tr}(\hat{\rho}\log\hat{\rho})$ reaching its largest value $S(\hat{\rho}^{(s)}) = \ln N$. In the absence of additional symmetries of $\hat{P}$, namely, for $\hat{P}^T \neq \hat{P}$, $\hat{\rho}^{(s)}$ is the only nondecaying eigenvector of $\mathcal{L}$: this means that, if the mean-field dynamics displays the NHSE, then the relaxation dynamics drives the system toward a maximally mixed state. However, when the system shows the additional symmetry $\hat{P}^T = \hat{P}$, corresponding to the absence of the NHSE in the mean-field limit, besides $\hat{\rho}^{(s)}$ there is *at least* another stationary state, given by $\hat{\rho}^{(s_a)}_{n,m} = (N+1)^{-1}(\delta_{n,m} + \delta_{n,N-n+1})$; technical details are given in [70]. We also mention that more than two stationary states can arise when $\hat{P}^T = \hat{P}$ and the matrices $\hat{P}$ and $\hat{H}$ are tridiagonal, i.e., when there are only nearest-neighbor hopping [like in model (3) with $T = 0$] [70]. This implies that, when the system possesses the symmetry $P(-k) = P(k)$ and the NHSE is prevented in the semiclassical limit, the dissipative process does not drive the system toward a maximally mixed state for rather arbitrary initial conditions, and the von Neumann entropy S remains below the value $\ln N$, as illustrated in Figs. 3 and 4. The long-time evolution of density matrix in a lattice with open boundaries, shown in Fig. 3 for the Hamiltonian (3) with $T = 0$, clearly indicates that the system relaxes to a maximally mixed state except for $\varphi = 0$. Such a behavior is closely related to the spectrum of the Liouvillian superoperator $\mathcal{L}$, which is shown in Fig. 4. While for $\varphi \neq 0$ the Liouvillian $\mathcal{L}$ has a single nondecaying stationary state, corresponding to the largest von Neumann entropy $S = \log N$, for $\varphi = 0$ there are N distinct stationary (nondecaying) states [64]. In the latter case the stationary state

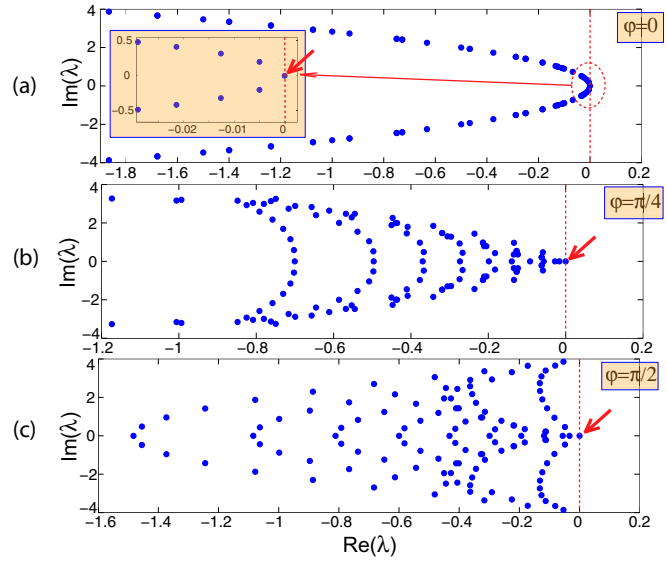

FIG. 4. Numerically computed eigenvalues λ of the Liouvillian superoperator $\mathcal{L}$ corresponding to the simulations of Fig. 3. The arrows show the zero eigenvalue of $\mathcal{L}$, which is simple in (b) and (c) and N-fold degenerate in (a).

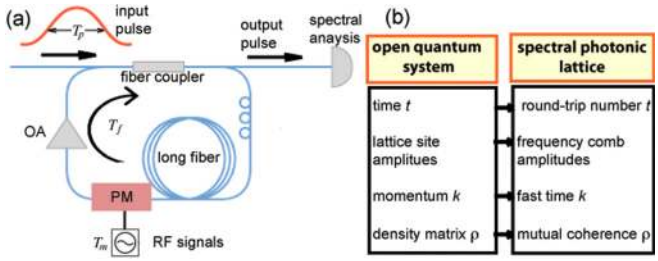

FIG. 5. (a) Setup of a spectral photonic lattice. An optical pulse circulating in a fiber loop containing an optical amplifier (OA) and a phase modulator (PM), driven by a period rf signal with stochastic amplitudes at successive transits, realizes the stochastic process (4) in frequency domain. (b) Equivalence between a dissipative quantum lattice and a spectral photonic lattice.

in the long-time limit depends on the initial state $\rho_{n,m}(0)$ of the system, and does not correspond rather generally to the maximally mixed state. Numerical diagonalization of $\mathcal{L}$ shows that, while for $\varphi \neq 0$ $\hat{H}_{eff}$ shows the NHSE, the eigenstates of $\mathcal{L}$ *are not* skin modes, i.e., we do not have here the Liouvillian skin effect [62]. We stress that in the one-band limit the presence of the NHSE in the semiclassical description and the relaxation toward a maximally mixed state in the master equation description have the same physical ground, i.e., breaking of the symmetry $P(-k) = P(k)$.

The above results are rather general ones and persist in one-band models with long-range hopping [e.g., $T \neq 0$ in Eq. (3)]. In the Supplemental Material [70] we discuss another example, the stochastic extension of the Hatano-Nelson model [1], which displays a long-range matrix $\hat{P}$.

Photonic simulation of stochastic dynamics. Classical systems with unitary dynamics driven by noise can provide a feasible platform to emulate the stochastic Schrödinger equation (4) with a collective jump operator. In such classical systems, decoherence arises by averaging over an ensemble of stochastic but unitary dynamics. A possible implementation in optics is provided by *spectral* photonic lattices [78–83]. A long light pulse circulating in a fiber loop with negligible dispersion and periodically kicked by a phase modulator realizes a spectral lattice where the spectral curves $H(k)$ and $P(k)$ in Eq. (4) are determined by the waveform that drives the modulator. A schematic of the photonic setup and the equivalence between a quantum dissipative lattice and a spectral photonic lattice are illustrated in Fig. 5. A long optical pulse with envelope $\Psi(k, 0)$ of temporal duration T_p is injected by an optical coupler into a long fiber loop, where k denotes the fast time. The transit time T_f of light in the loop is much longer than T_p and defines a slow time t (round-trip number) in such a way that the physical time τ is given by $\tau = tT_f + k$, with $t = 0, 1, 2, 3, \ldots$ and $0 < k < T_f$ [84]. A phase modulator impresses a periodic phase change $\Delta\theta_t(k) = H(k) + \xi_t P(k)$ to the optical pulse after each transit t in the loop, where the fast time k is given in units of the modulation period T_m and ξ_t are independent Gaussian variables with zero mean and unit variance, i.e., $\overline{\xi_t} = 0$ and $\overline{\xi_t \xi_{t'}} = \delta_{t,t'}$. An optical amplifier is placed inside the loop to compensate for the coupler losses. In this way, the envelope $\Psi(k, t)$ of the optical pulse at the tth transit in the loop reads

$$\Psi(k, t) = \Psi(k, 0) \exp[-iH(k)t - iP(k)W(t)], \qquad (9)$$

where $W(t) = \sum_{l=0}^{t} \xi_l$ is a stroboscopic map of a Wiener process at discrete times t, i.e., $\overline{W(t)} = 0$ and $\overline{W^2(t)} = t$. A comparison of Eqs. (6) and (9) shows that the pulse evolution at successive transits in the loop describes a stroboscopic map of a quantum trajectory in Bloch space of a dissipative quantum system with effective non-Hermitian Hamiltonian $H_{eff}(k) = H(k) - (i/2)P^2(k)$. The spectral content (frequency comb) $\psi_n(t) = \int dk\, \Psi(k, t) \exp(ikn)$ of the optical pulse at successive transits, which provides the site occupation amplitudes $\langle n|\psi(t)\rangle$ of the synthetic lattice, can be monitored at the output port of the coupler. The analog of the density matrix $\rho_{n,m}$ is the noise-averaged spectral matrix $\overline{\psi_n \psi_m^*}$, i.e., so-called mutual coherence or complex visibility [85,86], which can be measured by suitable techniques [86]. The short-time relaxation dynamics of density matrix, with the characteristic elongated pattern for $\varphi \neq 0$ shown in Fig. 2, could be thus accessed in the optical platform.

Conclusion. In this work we reconsidered a paradigmatic effect of non-Bloch band theory, the non-Hermitian skin effect, in the framework of open quantum systems. Our results reveal hidden signatures of the skin effect beyond the non-Hermitian theory, suggesting that quantities used in quantum statistical mechanics, such as von Neumann entropy, might provide a pivotal role in characterizing dissipative topological matter beyond semiclassical models. Noise-driven classical systems, such as stochastic-driven spectral photonic lattices, could provide a suitable platform for the observation of jump dynamics and hidden signatures of the skin effect.

Acknowledgments. The author acknowledges the Spanish State Research Agency through the Severo Ochoa and María de Maeztu Program for Centers and Units of Excellence in R&D (Grant No. MDM-2017-0711).

[1] N. Hatano and D. R. Nelson, Localization Transitions in Non-Hermitian Quantum Mechanics, Phys. Rev. Lett. **77**, 570 (1996).

[2] M. S. Rudner and L. S. Levitov, Topological Transition in a Non-Hermitian Quantum Walk, Phys. Rev. Lett. **102**, 065703 (2009).

[3] H. Schomerus, Topologically protected midgap states in complex photonic lattices, Opt. Lett. **38**, 1912 (2013).

[4] C. Poli, M. Bellec, U. Kuhl, F. Mortessagne, and H. Schomerus, Selective enhancement of topologically induced interface states in a dielectric resonator chain, Nat. Commun. **6**, 6710 (2015).

[5] S. Longhi, D. Gatti, and G. Della Valle, Non-Hermitian transparency and one-way transport in low-dimensional lattices by an imaginary gauge field, Phys. Rev B **92**, 094204 (2015).

[6] T. E. Lee, Anomalous Edge State in a Non-Hermitian Lattice, Phys. Rev. Lett. **116**, 133903 (2016).

[7] D. Leykam, K. Y. Bliokh, C. Huang, Y. D. Chong, and F. Nori, Edge Modes, Degeneracies, and Topological Numbers in Non-Hermitian Systems, Phys. Rev. Lett. **118**, 040401 (2017).

[8] X. Han, L. Xiao, Z. Bian, K. Wang, X. Qiu, B. C. Sanders, W. Yi, and P. Xue, Detecting Topological Invariants in Nonunitary Discrete-Time Quantum Walks, Phys. Rev. Lett. **119**, 130501 (2017).

[9] M. Pan, H. Zhao, P. Miao, S. Longhi, and L. Feng, Photonic zero mode in a non-Hermitian photonic lattice, Nat. Commun. **9**, 1308 (2018).

[10] H. Shen, B. Zhen, and L. Fu, Topological Band Theory for Non-Hermitian Hamiltonians, Phys. Rev. Lett. **120**, 146402 (2018).

[11] Z. Gong, Y. Ashida, K. Kawabata, K. Takasan, S. Higashikawa, and M. Ueda, Topological Phases of Non-Hermitian Systems, Phys. Rev. X **8**, 031079 (2018).

[12] Y. Xiong, Why does bulk boundary correspondence fail in some non-Hermitian topological models, J. Phys. Commun. **2**, 035043 (2018).

[13] F. K. Kunst, E. Edvardsson, J. C. Budich, and E. J. Bergholtz, Biorthogonal Bulk-Boundary Correspondence in Non-Hermitian Systems, Phys. Rev. Lett. **121**, 026808 (2018).

[14] S. Yao and Z. Wang, Edge States and Topological Invariants of Non-Hermitian Systems, Phys. Rev. Lett. **121**, 086803 (2018).

[15] V. M. Martinez Alvarez, J. E. Barrios Vargas, and L. E. F. Foa Torres, Non-Hermitian robust edge states in one dimension: Anomalous localization and eigenspace condensation at exceptional points, Phys. Rev. B **97**, 121401(R) (2018).

[16] S. Yao, F. Song, and Z. Wang, Non-Hermitian Chern Bands, Phys. Rev. Lett. **121**, 136802 (2018).

[17] C. H. Lee and R. Thomale, Anatomy of skin modes and topology in non-Hermitian systems, Phys. Rev. B **99**, 201103(R) (2019).

[18] A. Ghatak and T. Das, New topological invariants in non-Hermitian systems, J. Phys.: Condens. Matter **31**, 263001 (2019).

[19] K. Kawabata, K. Shiozaki, M. Ueda, and M. Sato, Symmetry and Topology in Non-Hermitian Physics, Phys. Rev. X **9**, 041015 (2019).

[20] H. Zhou and J. Y. Lee, Periodic table for topological bands with non-Hermitian Bernard-LeClair symmetries, Phys. Rev. B **99**, 235112 (2019).

[21] C.-H. Liu, H. Jiang, and S. Chen, Topological classification of non-Hermitian systems with reflection symmetry, Phys. Rev. B **99**, 125103 (2019).

[22] C. H. Lee, L. Li, and J. Gong, Hybrid Higher-Order Skin- Topological Modes in Non-Reciprocal Systems, Phys. Rev. Lett. **123**, 016805 (2019).

[23] E. Edvardsson, F. K. Kunst, and E. J. Bergholtz, Non-Hermitian extensions of higher-order topological phases and their biorthogonal bulk-boundary correspondence, Phys. Rev. B **99**, 081302(R) (2019).

[24] F. Song, S. Yao, and Z. Wang, Non-Hermitian Skin Effect and Chiral Damping in Open Quantum Systems, Phys. Rev. Lett. **123**, 170401 (2019).

[25] K. Yokomizo and S. Murakami, Bloch Band Theory for Non-Hermitian Systems, Phys. Rev. Lett. **123**, 066404 (2019).

[26] F. Song, S. Yao, and Z. Wang, Non-Hermitian Topological Invariants in Real Space, Phys. Rev. Lett. **123**, 246801 (2019).

[27] T. Liu, Y.-R. Zhang, Q. Ai, Z. Gong, K. Kawabata, M. Ueda, and F. Nori, Second-Order Topological Phases in Non-Hermitian Systems, Phys. Rev. Lett. **122**, 076801 (2019).

[28] S. Longhi, Topological Phase Transition in Non-Hermitian Quasicrystals, Phys. Rev. Lett. **122**, 237601 (2019).

[29] S. Longhi, Probing non-Hermitian skin effect and non-Bloch phase transitions, Phys. Rev. Res. **1**, 023013 (2019).

[30] H. Wang, J. Ruan, and H. Zhang, Non-Hermitian nodal-line semimetals with an anomalous bulk-boundary correspondence, Phys. Rev. B **99**, 075130 (2019).

[31] L. Li, C. H. Lee, and J. Gong, Geometric characterization of non-Hermitian topological systems through the singularity ring in pseudospin vector space, Phys. Rev. B **100**, 075403 (2019).

[32] L. Herviou, J. H. Bardarson, and N. Regnault, Defining a bulk-edge correspondence for non-Hermitian Hamiltonians via singular-value decomposition, Phys. Rev. A **99**, 052118 (2019).

[33] L. Jin and Z. Song, Bulk-boundary correspondence in non-Hermitian systems in one dimension with chiral inversion symmetry, Phys. Rev. B **99**, 081103(R) (2019).

[34] F. K. Kunst and V. Dwivedi, Non-Hermitian systems and topology: A transfer matrix perspective, Phys. Rev. B **99**, 245116 (2019).

[35] T. S. Deng and W. Yi, Non-Bloch topological invariants in a non-Hermitian domain-wall system, Phys. Rev. B **100**, 035102 (2019).

[36] K.-I. Imura and Y. Takane, Generalized bulk-edge correspondence for non-Hermitian topological systems, Phys. Rev. B **100**, 165430 (2019).

[37] R. Hamazaki, K. Kawabata, and M. Ueda, Non-Hermitian Many-Body Localization, Phys. Rev. Lett. **123**, 090603 (2019).

[38] N. Okuma and M. Sato, Topological Phase Transition Driven by Infinitesimal Instability: Majorana Fermions in Non-Hermitian Spintronics, Phys. Rev. Lett. **123**, 097701 (2019).

[39] J. Y. Lee, J. Ahn, H. Zhou, and A. Vishwanath, Topological Correspondence between Hermitian and Non-Hermitian Systems: Anomalous Dynamics, Phys. Rev. Lett. **123**, 206404 (2019).

[40] S. Longhi, Non-Bloch PT symmetry breaking in non-Hermitian photonic quantum walks, Opt. Lett. **44**, 5804 (2019).

[41] H. Zhao, X. Qiao, T. Wu, B. Midya, S. Longhi, and L. Feng, Non-Hermitian topological light steering, Science **365**, 1163 (2019).

[42] D. S. Borgnia, A. J. Kruchkov, and R.-J. Slager, Non-Hermitian Boundary Modes and Topology, Phys. Rev. Lett. **124**, 056802 (2020).

[43] X. Zhang and J. Gong, Non-Hermitian Floquet topological phases: Exceptional points, coalescent edge modes, and the skin effect, Phys. Rev. B **101**, 045415 (2020).

[44] S. Longhi, Non-Bloch-Band Collapse and Chiral Zener Tunneling, Phys. Rev. Lett. **124**, 066602 (2020).

[45] Z. Yang, K. Zhang, C. Fang, and J. Hu, Auxiliary generalized Brillouin zone method in non-Hermitian band theory, arXiv:1912.05499.

[46] N. Okuma, K. Kawabata, K. Shiozaki, and M. Sato, Topological Origin of Non-Hermitian Skin Effects, Phys. Rev. Lett. **124**, 086801 (2020).

[47] L. Xiao, T. Deng, K. Wang, G. Zhu, Z. Wang, W. Yi, and P. Xue, Observation of non-Hermitian bulk-boundary correspondence in quantum dynamics, Nat. Phys. **16**, 761 (2020).

[48] T. Helbig, T. Hofmann, S. Imhof, M. Abdelghany, T. Kiessling, L. W. Molenkamp, C. H. Lee, A. Szameit, M. Greiter, and R. Thomale, Generalized bulk-boundary correspondence in non-Hermitian topolectrical circuits, Nat. Phys. **16**, 747 (2020).

[49] X.-R. Wang, C.-X. Guo, and S.-P. Kou, Defective edge states and number-anomalous bulk-boundary correspondence in

non-Hermitian topological systems, Phys. Rev. B **101**, 121116(R) (2020).
[50] K. Kawabata, N. Okuma, and M. Sato, Non-Bloch band theory of non-Hermitian Hamiltonians in the symplectic class, Phys. Rev. B **101**, 195147 (2020).
[51] L. Li, C. H. Lee, and J. Gong, Topological Switch for Non-Hermitian Skin Effect in Cold-Atom Systems with Loss, Phys. Rev. Lett. **124**, 250402 (2020).
[52] A. Ghatak, M. Brandenbourger, J. van Wezel, and C. Coulais, Observation of non-Hermitian topology and its bulk-edge correspondence, arXiv:1907.11619.
[53] S. Weidemann, M. Kremer, T. Helbig, T. Hofmann, A. Stegmaier, M. Greiter, R. Thomale, and A. Szameit, Topological funneling of light, Science **368**, 311 (2020).
[54] T. Hofmann, T. Helbig, F. Schindler, N. Salgo, M. Brzezinska, M. Greiter, T. Kiessling, D. Wolf, A. Vollhardt, A. Kabai, C. H. Lee, A. Bilusic, R. Thomale, and T. Neupert, Reciprocal skin effect and its realization in a topolectrical circuit, Phys. Rev. Res. **2**, 023265 (2020).
[55] C. H. Lee and S. Longhi, Ultrafast and anharmonic Rabi oscillations between non-Bloch bands, Commun. Phys. **3**, 147 (2020).
[56] S. Lieu, M. McGinley, and N. R. Cooper, Tenfold Way for Quadratic Lindbladians, Phys. Rev. Lett. **124**, 040401 (2020).
[57] E. J. Bergholtz, J. C. Budich, and F. K. Kunst, Exceptional topology in non-Hermitian systems, arXiv:1912.10048.
[58] Y. Ashida, Z. Gong, and M. Ueda, Non-Hermitian physics, arXiv:2006.01837.
[59] S. Longhi, Stochastic non-Hermitian skin effect, Opt. Lett. **45**, 5250 (2020).
[60] L. Li, C. H. Lee, S. Mu, and J. Gong, Critical non-Hermitian skin effect, Nat. Commun. **11**, 5491 (2020).
[61] C. Gneiting, A. Koottandavida, A. V. Rozhkov, and F. Nori, Unraveling the topology of dissipative quantum systems, arXiv:2007.05960.
[62] T. Haga, M. Nakagawa, R. Hamazaki, and M. Ueda, Liouvillian skin effect: Slowing down of relaxation pprocesses without gap closing, arXiv:2005.00824.
[63] K. Zhang, Z. Yang, and C. Fang, Correspondence between Winding Numbers and Skin Modes in Non-Hermitian Systems, Phys. Rev. Lett. **125**, 126402 (2020).
[64] K. Kawabata, M. Sato, and K. Shiozaki, Higher-order non-Hermitian skin effect, arXiv:2008.07237.
[65] Y. Fu and S. Wan, Non-Hermitian second-order skin and topological modes, arXiv:2008.09033.
[66] S. Kalmykov and L. V. Kovalev, Self-intersections of Laurent polynomials and the density of Jordan curves, Proc. Am. Math. Soc. (to be published), https://doi.org/10.1090/proc/14594.
[67] F. Minganti, A. Miranowicz, R. W. Chhajlany, and F. Nori, Quantum exceptional points of non-Hermitian Hamiltonians and Liouvillians: The effects of quantum jumps, Phys. Rev. A **100**, 062131 (2019).
[68] F. Minganti, A. Miranowicz, R. W. Chhajlany, I. I. Arkhipov, and F. Nori, Hybrid-Liouvillian formalism connecting exceptional points of non-Hermitian Hamiltonians and Liouvillians via postselection of quantum trajectories, Phys. Rev. A **101**, 062112 (2020).
[69] N. G. van Kampe, *Stochastic processes in physics and chemistry* (Elsevier Science B. V., Amsterdam, North Holland, 2003).
[70] See the Supplemental Material at http://link.aps.org/supplemental/10.1103/PhysRevB.102.201103 for technical details regarding the following: (i) collective jump model and mean-field limit of stochastic Schrödinger equation and Lindblad master equation; (ii) relaxation dynamics; and (iii) the dissipative Hatano-Nelson model.
[71] C. W. Gardiner, *Handbook of stochastic methods* (Springer, Berlin, 1985).
[72] A. Eisfeld and J. S. Briggs, Classical master equation for excitonic transport under the influence of an environment, Phys. Rev. E **85**, 046118 (2012).
[73] S. Mukherjee, D. Mogilevtsev, G. Ya. Slepyan, T. H. Doherty, R. R. Thomson, and N. Korolkova, Dissipatively coupled waveguide networks for coherent diffusive photonics, Nat. Commun. **8**, 1909 (2017).
[74] T. Neuschel, Apéry polynomials and the multivariate saddle point method, Constr. Approx. **40**, 487 (2014).
[75] V. V. Albert and L. Jang, Symmetries and conserved quantities in Lindblad master equations, Phys. Rev. A **89**, 022118 (2014).
[76] F. Minganti, A. Biella, N. Bartolo, and C. Ciuti, Spectral theory of Liouvillians for dissipative phase transitions, Phys. Rev. A **98**, 042118 (2018).
[77] D. Manzano and P. I. Hurtado, Harnessing symmetry to control quantum transport, Adv. Phys. **67**, 1 (2018).
[78] L. Yuan, Y. Shi, and S. Fan, Photonic gauge potential in a system with a synthetic frequency dimension, Opt. Lett. **41**, 741 (2016).
[79] B. A. Bell, K. Wang, A. S. Solntsev, D. N. Neshev, A. A. Sukhorukov, and B. J. Eggleton, Spectral photonic lattices with complex long-range coupling, Optica **4**, 1433 (2017).
[80] L. Yuan, Q. Lin, M. Xiao, and S. Fan, Synthetic dimension in photonics, Optica **5**, 1396 (2018).
[81] C. Qin, F. Zhou, Y. Peng, D. Sounas, X. Zhu, B. Wang, J. Dong, X. Zhang, A. Alú, and P. Lu, Spectrum Control through Discrete Frequency Diffraction in the Presence of Photonic Gauge Potentials, Phys. Rev. Lett. **120**, 133901 (2018).
[82] A. Dutt, M. Minkov, Q. Lin, L. Yuan, D. A. B. Miller, and S. Fan, Experimental band structure spectroscopy along a synthetic dimension, Nat. Commun. **10**, 3122 (2019).
[83] C. Qin, B. Wang, Z. J. Wong, S. Longhi, and P. Lu, Discrete diffraction and Bloch oscillations in non-Hermitian frequency lattices induced by complex photonic gauge fields, Phys. Rev. B **101**, 064303 (2020).
[84] B. Fischer, A. Rosen, and S. Fishman, Localization in frequency for periodically kicked light propagation in a dispersive single-mode fiber, Opt. Lett. **24**, 1463 (1999).
[85] L. Mandel and E. Wolf, Spectral coherence and the concept of cross-spectral purity, J. Opt. Soc. Am. **66**, 529 (1976).
[86] J. G. Titchener, B. Bell, K. Wang, A. S. Solntsev, B. J. Eggleton, and A. A. Sukhorukov, Synthetic photonic lattice for single-shot reconstruction of frequency combs, APL Photonics **5**, 030805 (2020).